Response of a core coherent density oscillation on electron cyclotron resonance heating in Heliotron J plasma

Cite as: Phys. Plasmas **25**, 012513 (2018); https://doi.org/10.1063/1.5007903
Submitted: 04 October 2017 • Accepted: 12 January 2018 • Published Online: 29 January 2018

T. Kobayashi, S. Kobayashi, X. X. Lu, et al.

Response of a core coherent density oscillation on electron cyclotron resonance heating in Heliotron J plasma

T. Kobayashi,[1,a)] S. Kobayashi,[2] X. X. Lu,[3] N. Kenmochi,[4] K. Ida,[1] S. Ohshima,[2] S. Yamamoto,[2] S. Kado,[2] D. Kokubu,[3] K. Nagasaki,[2] H. Okada,[2] T. Minami,[2] Y. Otani,[3] and T. Mizuuchi[2]

[1]*National Institute for Fusion Science, National Institutes of Natural Sciences, Toki, Gifu 509-5292, Japan*
[2]*Institute of Advanced Energy, Kyoto University, Uji, Kyoto 611-0011, Japan*
[3]*Graduate School of Energy Science, Kyoto University, Uji, Kyoto 611-0011, Japan*
[4]*Graduate School of Frontier Sciences, The University of Tokyo, Kashiwa, Chiba 277-8561, Japan*

(Received 4 October 2017; accepted 12 January 2018; published online 29 January 2018)

We report properties of a coherent density oscillation observed in the core region and its response to electron cyclotron resonance heating (ECH) in Heliotron J plasma. The measurement was performed using a multi-channel beam emission spectroscopy system. The density oscillation is observed in a radial region between the core and the half radius. The poloidal mode number is found to be 1 (or 2). By modulating the ECH power with 100 Hz, repetition of formation and deformation of a strong electron temperature gradient, which is likely ascribed to be an electron internal transport barrier, is realized. Amplitude and rotation frequency of the coherent density oscillation sitting at the strong electron temperature gradient location are modulated by the ECH, while the poloidal mode structure remains almost unchanged. The change in the rotation velocity in the laboratory frame is derived. Assuming that the change of the rotation velocity is given by the background $E \times B$ velocity, a possible time evolution of the radial electric field was deduced. *Published by AIP Publishing.*
https://doi.org/10.1063/1.5007903

I. INTRODUCTION

Spontaneous confinement transition in magnetically confined plasmas has been intensively investigated because of its capability for reaching high plasma performance. Numerous studies have clarified that the transport barrier is formed when the confinement transition occurs, in which anomalous cross-field transport is suppressed by inhomogeneous $E \times B$ flow structures.[1] Tokamaks and heliotrons/stellarators share a typical confinement transition, the so-called electron internal transport barriers (e-ITBs).[2–8] For the case of heliotron/stellarator e-ITB, it is believed that the neoclassical radial electric field bifurcation occurs between the electron-root and the ion-root that forms a strong radial electric field shear.[4–6,8]

Interrelation between transport barriers and coherent fluctuations has attracted interest. For instance, an important role of the so-called edge harmonic oscillation in the quiescent-H-mode formation is revealed in tokamaks.[9,10] In the I-mode confinement regime, a weakly coherent mode that is considered to maintain the decoupling of the particle transport and the thermal transport is routinely observed.[11,12] Regarding the e-ITB, low frequency magnetohydrodynamic (MHD) modes are known to have an impact on the e-ITB dynamics through triggering, quenching, or giving saturations.[2,3,7] In order to properly control the e-ITBs for achieving high performance plasmas, it is crucial to predict the MHD activity in the e-ITB plasmas. In general, the magnetic configuration strongly impacts both the e-ITB formation and the MHD activity. In order to specify which aspect of the magnetic configuration is essential, case studies in different heliotron/stellarator devices having different configuration parameters, e.g., the magnetic shear or the magnetic well, are highly desirable for future multi-device comparison. Furthermore, comparisons between cases in tokamaks and heliotrons/stellarators are of great interest.

In this paper, we report the observation of a coherent density oscillation observed in the core region in Heliotron J plasmas by use of a multi-channel beam emission spectroscopy (BES) system.[13] The density oscillation is observed in a radial region between the core and the half radius. The poloidal mode number is found to be 1 (or 2). Repetition of formation and deformation of strong electron temperature gradient, which is likely ascribed to be an e-ITB, is realized by modulating the **electron cyclotron resonance heating** (ECH) power with 100 Hz. Amplitude and rotation frequency of the coherent density oscillation sitting at the strong electron temperature gradient location are modulated by the ECH, while the poloidal mode structure remains almost unchanged. The change in the coherent density oscillation rotation velocity in the laboratory frame is derived, from which the time evolution of the expected radial electric field is deduced.

II. EXPERIMENTAL SETUP

A. Heliotron J

Heliotron J is a helical-axis heliotron device having an averaged plasma major radius of $R = 1.2$ m and an averaged plasma minor radius of $a = 0.17$ m.[14] The target plasmas are sustained by two neutral beam injections (NBIs) of a total of 600 kW and an electron cyclotron resonance heating (ECH)

[a)]E-mail: kobayashi.tatsuya@LHD.nifs.ac.jp

of 48 kW. Above the stationary ECH, a square wave modulation of ECH power (the frequency of 100 Hz and a peak-top-peak amplitude of 194 kW) is superimposed that causes the formation/deformation of the strong electron temperature gradient. The modulation part of the ECH is called the modulation ECH (MECH). Both the stationary ECH and the MECH are injected toward on-axis. Ray-tracing code confirms that more than 77% of the total absorption power is deposited in $\rho < 0.3$. Toroidal magnetic field strength at the magnetic axis is $B_t = 1.23$ T. The magnetic configuration is characterized by a nearly flat vacuum rotational transform with the core value of $\iota_{core}/2\pi = 0.56$. Since Heliotron J has a low magnetic shear, low order rational surfaces do not exist in the vacuum configuration.

B. Beam emission spectroscopy

The local density fluctuation is measured with a multichannel beam emission spectroscopy (BES) system.[13] The line of sight for the BES system is designed to be almost parallel to the magnetic field line, which minimizes the line integration of the density fluctuation. In this experiment, an 8×2 rectangular array of sampling volumes (radial direction $\times$ vertical direction) is composed to diagnose the two-dimensional fluctuation structure at the mid-plane of the high field side of the torus. The spatial resolution is approximately 1 cm and the sampling time is 1 μs. The upper limit of the detectable frequency of density oscillation is 200 kHz, which is determined by the cut-off frequency of the amplifier. The sampling volumes cover the plasma core region, $0.1 < \rho < 0.5$, where $\rho = r/a$ is the normalized averaged minor radius and r is the averaged minor radius.

III. EXPERIMENTAL RESULTS

A. Target discharges

Figure 1 show the time evolutions of (a) the heating power, (b) the line averaged density, (c) the plasma stored energy, and [(d) and (e)] the electron temperature measured by the ECE radiometer at the core region, $\rho \sim 0.33$, and the edge region, $\rho \sim 0.67$, respectively. The ECE signal is calibrated using the electron temperature profile measured by the Thomson scattering system.[15] Data from different discharges (#61280–#61285) having an excellent reproducibility are overplotted. With the modulation frequency of the MECH (100 Hz), the plasma parameters are modulated. In particular, the core electron temperature shows a large modulation amplitude of $\delta T_e \sim 0.25$ keV, whereas the edge temperature modulation is moderate.

Figure 2 is the electron temperature profile measured by the Thomson scattering system when the MECH is turned on and turned off, respectively. In order to increase the signal to noise ratio, data from different discharges are averaged. The horizontal axis ρ_{vac} denotes the normalized averaged minor radius in the vacuum magnetic surface. During the discharge, the plasma center slightly shifts outward due to a finite plasma beta. A strong electron temperature gradient is formed when the MECH is turned on, which is likely ascribed to the e-ITB.[8] A repetition of formation and deformation of the strong electron temperature gradient occurs with the MECH frequency. A radius in which the improved confinement region and the normal confinement region are connected, which we call the connection radius, exists at $\rho \sim 0.3$. When the MECH is turned off and only the stationary ECH is injected, the heating power is not sufficient to reach the improved confinement. In that case, the temperature profile is rather smooth and the discontinuity in the temperature gradient does not appear, as shown by the black curve in Fig. 2.

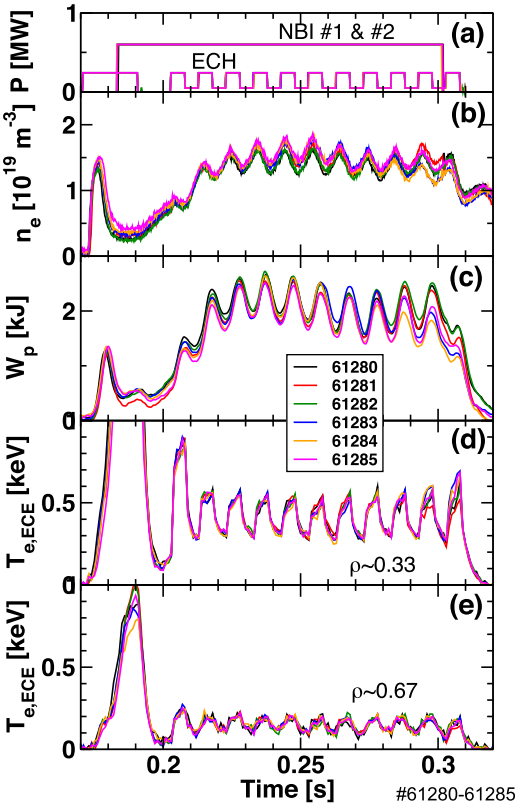

FIG. 1. Time evolution of (a) heating power (the ECH is mainly absorbed in $\rho < 0.3$), (b) line averaged density, (c) plasma stored energy, and electron temperature measured by the ECE radiometer in (d) the core region ($\rho \sim 0.33$) and (e) the edge region ($\rho \sim 0.67$).

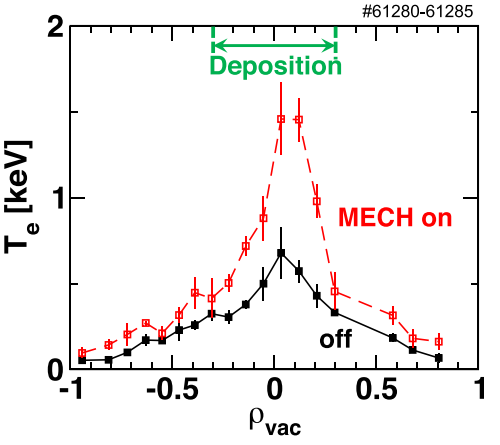

FIG. 2. Electron temperature profile measured by the Thomson scattering system when the MECH is turned on and turned off.

B. Core coherent density oscillation

The response of the density fluctuation to the MECH and/or the electron temperature gradient formation is measured by the BES system. Figure 3(a) is the time evolution of the density fluctuation wavelet spectrum measured at $\rho \sim 0.28$ close to the connection radius. In the second half of the discharge, $0.24\,\mathrm{s} < t < 0.30\,\mathrm{s}$, a sharp peak appears quasi-intermittently in the frequency spectrum. The central frequency of the peak is found to vary with the ECH power modulation. Figure 3(c) is the time averaged spectrum when the MECH is turned on and turned off. The central frequency of the quasi-coherent oscillation is $\sim$7 kHz and $\sim$15 kHz when the MECH is turned on and turned off, respectively.

In order to compare the properties of the coherent density oscillation when the MECH is turned on and off, background noise and/or incoherent density fluctuations are removed by means of the conditional averaging technique. Here, the ensembles are taken not only from different periods of the MECH but also from different discharges, which results in a total of 24 ensembles of the event. The time dependent cross spectrum is defined as

$$\bar{S}_{1,2}(\tau,f) = \frac{1}{N}\sum_{i=1}^{N} W_1(t_i+\tau,f)W_2^*(t_i+\tau,f), \qquad (1)$$

where $W_1(t_i+\tau,f)$ and $W_2(t_i+\tau,f)$ are the wavelet spectrum of density fluctuation signals from the vertically separated BES channels. The asterisk in Eq. (1) denotes the complex conjugate. The time instance t_i indicates the i-th MECH turn on time, N is the total number of the modulation, and $-T/2 < \tau \le T/2$ where T is the time period of the MECH. Figure 4(b) shows the absolute value of the conditional averaged cross spectrum of vertically separated BES channels at $\rho \sim 0.28$. The time dependent dynamics of the fluctuation spectrum is clearly captured. The frequency immediately responds upon the MECH turning on with the time scale of approximately 1 ms or less. A few milliseconds after, the central frequency is no longer robust, and a back transition event likely occurs. When the MECH is turned off, a decrease of the central frequency occurs with, possibly, a slightly longer time scale than the case of the MECH turning on.

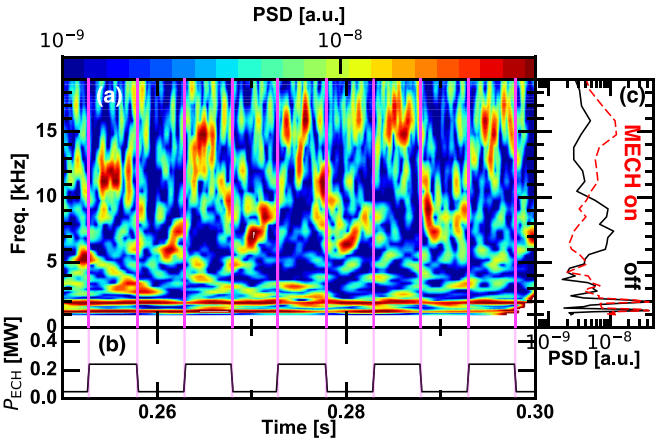

FIG. 3. Time evolution of (a) density fluctuation spectrum at $\rho \sim 0.28$ measured with the BES and (b) ECH power, and (c) time averaged spectrum when the MECH is turned on and turned off. Vertical lines in (a) and (b) provide eye-guides for ECH turn-on time and turn-off time.

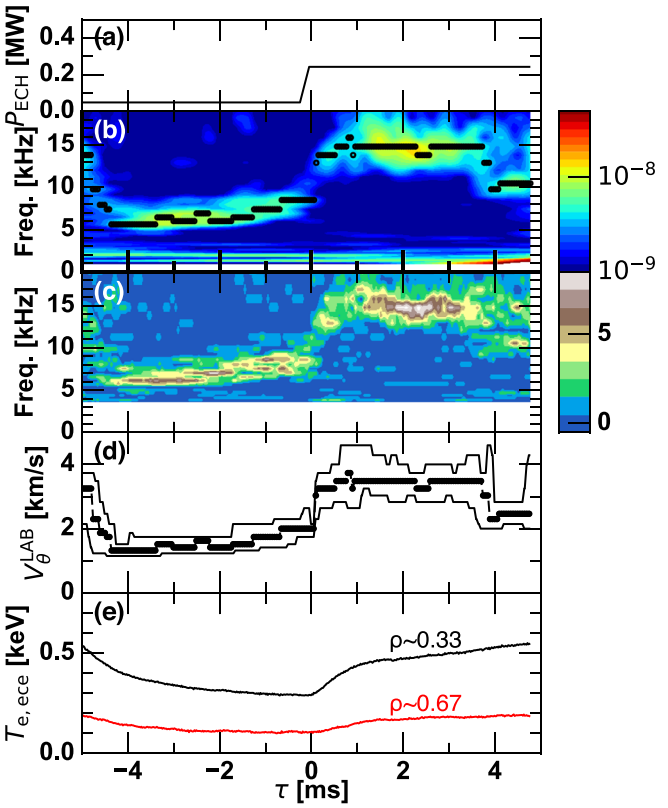

FIG. 4. Conditional averaged (a) ECH power, (b) power spectrum in density fluctuation measured with the BES, (c) probability density function (PDF) of the peak frequency as a function of the reference time τ, (d) evaluated poloidal rotation velocity of the mode in the laboratory frame, and (e) electron temperature at $\rho \sim 0.33$ and $\rho \sim 0.67$. Black dots in (b) show the local peak of the spectrum.

The use of the conditional averaging is valid when statistical properties of all ensembles follow the Gaussian distribution. In order to confirm this point, the probability density function (PDF) of the peak frequency is analyzed. The PDF is obtained from the 24 sets of the time evolution of the peak frequency as a function of τ. The PDF plotted in Fig. 4(c) shows the most probable time evolution of the peak frequency. The fast change in the peak frequency shown in Fig. 4(b) is confirmed statistically as well. Although the number of ensembles is not sufficiently large to discuss the shape of the distribution function, it is confirmed that the time evolutions of the peak frequency follow a symmetric distribution without a large deviation.

C. Spatial structure of the core coherent density oscillation

The spatial structure of the core coherent density oscillation is investigated in detail. Figure 5 shows the radial profile of (a) the mode amplitude, (b) the cross coherence γ^2, and (c) the poloidal mode number obtained from the pair of vertically separated BES channels. The amplitude is defined as the square root of the absolute value of the cross spectrum. The poloidal mode number is obtained as $m = \Delta\theta r/d$, where

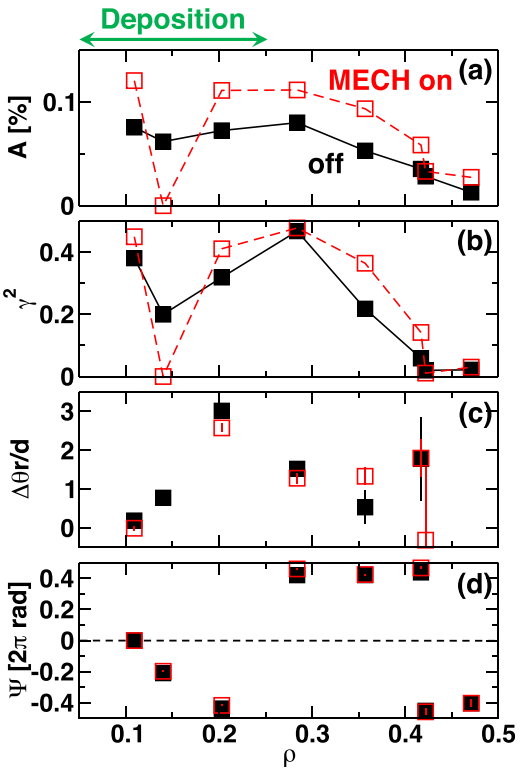

FIG. 5. Radial profile of (a) amplitude, (b) cross coherence from the pair of vertical channels, (c) poloidal mode number, and (d) radial phase difference from the core BES signal of the coherent density oscillation. The ECH is mainly absorbed in $\rho < 0.3$, and the connection radius of the electron temperature gradient exists at $\rho \sim 0.3$.

$\Delta\theta$ is the phase difference and $d \sim 1$ cm is the distance between two vertical channels. The positive value of m corresponds to the mode rotating in the ion diamagnetic direction. When the MECH is turned on and the strong electron temperature gradient is formed, the mode amplitude and the cross coherence slightly increase. The poloidal mode number structure remains almost unchanged. Although the evaluated poloidal mode number is not constant in radius, it is natural to regard that the mode is rotating rigidly because the cross coherence among signals from radially separated BES channels are high (not shown). In this case, the most plausible poloidal mode number might be $m = 1$ or 2. Heliotron J plasma has a low shear rotational transform of $\iota/2\pi \sim 0.56$ even with a nonzero toroidal current ascribed to the neutral beam current drive and/or the bootstrap current.[16] Considering a resonant MHD mode with a finite toroidal mode number, $m = 1$ oscillation seems unlikely unless $\iota/2\pi \sim 1$ is satisfied. Note that a different set of discharges having a half line averaged density shows a signature of $m = 2$ oscillation in the similar situation. Note also that the mode in the present set of discharges does not show a clear coherence with the on-vessel magnetic probe signal, which may be due to a relatively large distance between the radius where the mode exists and the magnetic probes. The radial phase difference from the core BES signal $\Psi_r(r)$ is shown in Fig. 5(d). A smooth phase inversion occurs between the core region and $\rho \sim 0.3$. A similar observation is given in Ref. 17.

Using the measured information, the spatial structure of the mode is reconstructed in the poloidal cross section. It is defined as

$$I(r, \theta) = A(r) \cos [\Psi_r(r) + m\theta], \tag{2}$$

where $A(r)$ and $\Psi_r(r)$ indicate the amplitude and the phase difference of the mode given in Figs. 5(a) and 5(d), respectively. Here, we take $m = 1$ for the poloidal mode number according to the discussions above. Figure 6 shows the reconstructed spatial structure in (a) the MECH turning off phase and (b) the MECH turning on phase. After the MECH is turned on, the strong electron temperature gradient is formed and the rotation frequency increases without any major change of the mode structure.

Although the identification of the coherent density oscillation is out of the scope of this paper, we attempt to raise possible candidates of the density oscillation. The first candidate would be a MHD instability in the core region. In some similar discharges, a weak correlation between the BES signal and the on-vessel magnetic probe signal was obtained. Energetic particle driven modes[18] cannot be excluded as well since the two NBIs supply the source of the mode excitation energy. Another candidate is the so-called long-range fluctuation nonlinearly driven by turbulence, which has been observed in the LHD experiment.[19]

IV. DISCUSSION

Here, we attempt to interpret the cause of the frequency change of the core coherent density oscillation. Change in the mode rotation velocity in the laboratory frame, V_θ^{LAB}, is derived as

$$V_\theta^{\mathrm{LAB}} = 2\pi fr/m. \tag{3}$$

With the global low frequency oscillation, the low order poloidal and toroidal mode numbers, m and n, respectively, are expected. Since the major radius and the minor radius have an order of magnitude difference, the poloidal wavenumber is considered to be much larger than the toroidal wavenumber. Under such a condition, change in the mode rotation frequency is sensitive to change in the poloidal velocity rather than the toroidal velocity. The time evolution

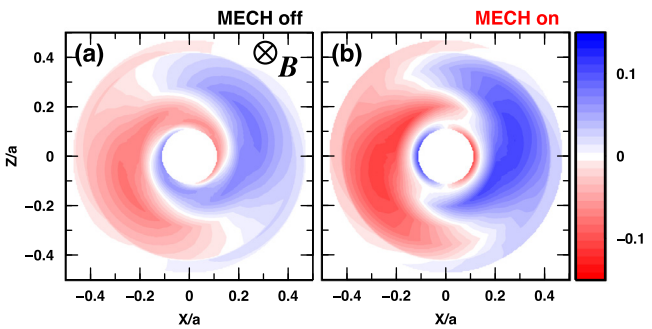

FIG. 6. Reconstructed mode structure in the poloidal cross section in (a) MECH turned off phase and (b) MECH turned on phase. Axes X/a and Z/a represent the horizontal distance and the vertical distance from the magnetic axis normalized by the plasma averaged minor radius, respectively.

of the mode frequency f is obtained from Fig. 4(b). Figure 4(d) shows the time evolution of the mode rotation velocity in the laboratory frame V_θ^{LAB} at $\rho = 0.28$. Two thinner curves indicate the frequency width at the half maximum of the spectral peak. The conditional averaged electron temperature at $\rho \sim 0.33$ and $\rho \sim 0.67$ measured by the ECE system is plotted in Fig. 4(e). By applying the MECH, the mode is accelerated in the ion diamagnetic direction. The change in the mode rotation velocity starts just after the MECH is turned on. The mode rotation velocity saturates earlier than the electron temperature.

As a working hypothesis, we assume that this change is driven by the change in the background $E \times B$ rotation velocity. The expected radial electric field is given as $E_r = V_\theta^{\mathrm{LAB}} B_{\mathrm{t}}$. A similar method for the rotation velocity estimation is widely used by means of movement of turbulence pattern measured with imaging-BES systems or other imaging diagnostics, which is sometimes called the "velocimetry". See Ref. 20. Note that the contributions from the ion pressure gradient and the toroidal rotation velocity in the radial force balance equation are considered to play minor roles with the modulation of the ECH. Change in the radial electric field is estimated to be approximately $+2$ kV/m.

Referring to the case of the e-ITB formation in the ECH sustained plasma,[8] the expected change in the radial electric field from the neoclassical theory is $O(+1)$ kV/m at $\rho \sim 0.3$ in the electron root solution. The magnitude of the E_r change in the present evaluation is in the same order with the case of the e-ITB formation in the ECH plasma, although the plasma properties in the NBI plasma and ECH plasma are not identical. Therefore, the increase of the neoclassical radial electric field in the electron root by applying the MECH would be a possible explanation for the stronger positive E_r excitation. The larger the electron temperature reaches, the greater the positive radial electric field is formed, which likely contributes further suppression of the turbulent transport. The observed time scale of the transition may correspond to the time scale of this feed-back loop for the square wave modulation. It should be noted that we did not take into account the intrinsic propagation velocity of the mode, which is unknown. If the change in the intrinsic mode velocity in response to the MECH is larger than the change in background $E \times B$ velocity, the above evaluation is no longer valid.

V. SUMMARY

We reported the observation of a core coherent density oscillation in Heliotron J plasmas by use of a multi-channel beam emission spectroscopy (BES) system. The density oscillation was observed in a radial region between the core and the half radius. The poloidal mode number was found to be 1 (or 2). Repetition of a strong electron temperature gradient formation/deformation was realized by modulating the ECH power with 100 Hz. Amplitude and rotation frequency sitting at the strong electron temperature gradient location were modulated by the ECH, while the mode structure was nearly unchanged. The change in the mode rotation velocity in the laboratory frame was derived, from which a possible time evolution of the radial electric field was deduced.

ACKNOWLEDGMENTS

The authors wish to thank the members of the Heliotron J group for their assistance in conducting the experiments. One of the authors (T.K.) thanks Professor S. Sakakibara for strong support. This work was partly supported by the Grant-in-Aid for Scientific Research of JSPS (17K14898), the collaboration programs of NIFS and Kyoto University (NIFS17KUHL075), and the Joint Usage/Research Program on Zero-Emission Energy Research, Institute of Advanced Energy, Kyoto University (ZE28B-11).

[1]P. H. Diamond, S.-I. Itoh, K. Itoh, and T. S. Hahm, Plasma Phys. Controlled Fusion **47**, R35 (2005).
[2]K. A. Razumova, V. V. Alikaev, A. A. Borschegovskii, V. V. Chistyakov, M. M. Dremin, A. V. Gorshkov, A. Ya Kislov, D. A. Kislov, S. V. Krylov, S. E. Lysenko *et al.*, Plasma Phys. Controlled Fusion **42**, 973 (2000).
[3]E. Joffrin, C. D. Challis, T. C. Hender, D. F. Howell, and G. T. A. Huysmans, Nucl. Fusion **42**, 235 (2002).
[4]A. Fujisawa, H. Iguchi, T. Minami, Y. Yoshimura, H. Sanuki, K. Itoh, S. Lee, K. Tanaka, M. Yokoyama, M. Kojima *et al.*, Phys. Rev. Lett. **82**, 2669 (1999).
[5]U. Stroth, K. Itoh, S.-I. Itoh, H. Hartfuss, H. Laqua, the ECRH team, and the W7-AS team, Phys. Rev. Lett. **86**, 5910 (2001).
[6]K. Ida, T. Shimozuma, H. Funaba, K. Narihara, S. Kubo, S. Murakami, A. Wakasa, M. Yokoyama, Y. Takeiri, K. Y. Watanabe *et al.*, Phys. Rev. Lett. **91**, 085003 (2003).
[7]T. Estrada, D. López-Bruna, A. Alonso, E. Ascasíbar, A. Baciero, A. Cappa, F. Castejón, A. Fernández, J. Herranz, C. Hidalgo *et al.*, Fusion Sci. Technol. **50**, 127–135 (2006).
[8]N. Kenmochi, T. Minami, C. Takahashi, S. Mochizuki, K. Nishioka, S. Kobayashi, K. Nagasaki, Y. Nakamura, H. Okada, S. Kado *et al.*, Plasma Phys. Controlled Fusion **59**, 055013 (2017).
[9]K. H. Burrell, T. H. Osborne, P. B. Snyder, W. P. West, M. E. Fenstermacher, R. J. Groebner, P. Gohil, A. W. Leonard, and W. M. Solomon, Phys. Rev. Lett. **102**, 155003 (2009).
[10]W. Suttrop, G. D. Conway, L. Fattorini, L. D. Horton, T. Kurki-Suonio, C. F. Maggi, M. Maraschek, H. Meister, R. Neu, Th. Pütterich *et al.*, Plasma Phys. Controlled Fusion **46**, A151 (2004).
[11]D. G. Whyte, A. E. Hubbard, J. W. Hughes, B. Lipschultz, J. E. Rice, E. S. Marmar, M. Greenwald, I. Cziegler, A. Dominguez, T. Golfinopoulos *et al.*, Nucl. Fusion **50**, 105005 (2010).
[12]P. Manz, Ph. Lauber, V. E. Nikolaeva, T. Happel, F. Ryter, G. Birkenmeier, A. Bogomolov, G. D. Conway, M. E. Manso, M. Maraschek *et al.*, Nucl. Fusion **55**, 083004 (2015).
[13]S. Kobayashi, S. Kado, T. Oishi, S. Ohshima, T. Kagawa, Y. Nagae, S. Yamamoto, T. Mizuuchi, K. Nagasaki, H. Okada *et al.*, Rev. Sci. Instrum. **83**, 10D535 (2012).
[14]T. Obiki, T. Mizuuchi, K. Nagasaki, H. Okada, F. Sano, K. Hanatani, Y. Liu, T. Hamada, Y. Manabe, H. Shidara *et al.*, Nucl. Fusion **41**, 833 (2001).
[15]N. Kenmochi, T. Minami, C. Takahashi, S. Tei, T. Mizuuchi, S. Kobayashi, K. Nagasaki, Y. Nakamura, H. Okada, S. Kado *et al.*, Rev. Sci. Instrum. **85**, 11D819 (2014).
[16]G. Motojima, S. Yamamoto, H. Okada, S. Sakakibara, K. Y. Watanabe, K. Nagasaki, Y. Suzuki, T. Mizuuchi, S. Kobayashi, B. D. Blackwell *et al.*, Plasma Fusion Res. **3**, S1067–S1067 (2008).
[17]M. Kirimoto, "Wavenumber spectrum analysis of density fluctuation using beam emission spectroscopy on Heliotron J," Master's thesis (Kyoto University, 2015) (in Japanese).
[18]S. Yamamoto, K. Nagasaki, Y. Suzuki, T. Mizuuchi, H. Okada, S. Kobayashi, B. Blackwell, K. Kondo, G. Motojima, N. Nakajima *et al.*, Fusion Sci. Technol. **51**, 92–96 (2007).
[19]S. Inagaki, T. Tokuzawa, K. Itoh, K. Ida, S.-I. Itoh, N. Tamura, S. Sakakibara, N. Kasuya, A. Fujisawa, S. Kubo *et al.*, Phys. Rev. Lett. **107**, 115001 (2011).
[20]G. McKee, R. Fonck, D. Gupta, D. Schlossberg, M. Shafer, R. Boivin, and W. Solomon, Plasma Fusion Res. **2**, S1025 (2007).